

---

## FLEX-THEORY FOR HIGH- $T_C$ SUPERCONDUCTIVITY DUE TO SPIN FLUCTUATIONS

---

D. MANSKE AND K.H. BENNEMANN

*Institut für Theoretische Physik, Arnimallee 14, D-14195 Berlin, Germany*

*E-mails: dmanske@physik.fu-berlin.de, khb@physik.fu-berlin.de*

Using the Hubbard model we develop a microscopic theory for high-temperature superconductivity due to the exchange of antiferromagnetic spin fluctuations. We treat the corresponding pairing mechanism self-consistently within the framework of the FLuctuation EXchange (FLEX) approximation and study some extensions. Solving the generalized Eliashberg equations for hole- and electron-doped superconductors we obtain both phase diagrams, respectively, and always a  $d$ -wave gap function. Furthermore, for hole-doped cuprates we find three characteristic temperature scales which are in qualitative agreement with the experimental situation: a pseudogap temperature  $T^*$ , below which a gap opens in the density of states, a mean-field transition temperature  $T_c^*$  for superconductivity below which we obtain Cooper-pairs without long-range phase coherence (“pre-formed Cooper-pairs”), and a critical temperature  $T_c$ , where these pairs become phase coherent.

### 1 Introduction

One of the most important and fascinating fields in condensed matter physics is the appearance of unconventional superconductivity, in particular high- $T_c$  superconductivity, in which the underlying mechanism is still under debate, even 15 years after the discovery by Bednorz and Müller [1]. In hole-doped superconductors the highest transition temperature  $T_c$  (without applying pressure), namely  $T_c = 133$  K, has been measured in  $\text{HgBa}_2\text{Ca}_2\text{Cu}_3\text{O}_{8+\delta}$ , followed by (to name just a few)  $\text{Bi}_2\text{Sr}_2\text{CaCu}_2\text{O}_{8+\delta}$  ( $\delta = 0.15 \leftrightarrow T_c = 95$  K),  $\text{YBa}_2\text{Cu}_3\text{O}_{7-\delta}$  ( $x = 0.93 \leftrightarrow T_c = 93$  K), and  $\text{La}_{2-x}\text{Sr}_x\text{CuO}_4$  where for a doping concentration  $x = 0.15$ , a maximum value of  $T_c = 39$  K occurs.

While hole-doped superconductors have been studied intensively the analysis of electron-doped cuprates remains largely unclear. Of course, it is of high

interest to see whether the behavior of hole-doped and electron-doped cuprate superconductors can be explained within a unified physical picture using for example the exchange of antiferromagnetic spin fluctuations as the relevant pairing mechanism. If Cooper-pairing is controlled by antiferromagnetic spin fluctuation one expects on general physical grounds that *d*-wave symmetry pairing should also occur for electron-doped cuprates. Previous experiments have not clearly supported this, reporting mainly *s*-wave pairing [2,3]. Maybe as a result, so far electron-doped cuprates received much less attention than hole-doped cuprates. However, recently phase sensitive experiments [4] and magnetic penetration depth measurements [5,6] exhibited *d*-wave symmetry Cooper-pairing also for electron-doped cuprates.

In general, all high- $T_c$  superconductors discovered so far contain  $\text{CuO}_2$ -planes and various metallic elements. Hence, they are often called cuprates. Their crystal structure resembles that of the perovskites. It is now mainly established that the relevant physics related to superconductivity occurs in the  $\text{CuO}_2$ -planes and that the other layers simply act as charge-reservoirs. Thus, the coupling in the *c*-direction provides a three-dimensional superconducting state but the main pairing interaction acts between carriers within a  $\text{CuO}_2$ -plane. As mentioned above,  $T_c$  for hole-doped cuprates is of the order of 100 K and thus much larger than in conventional strong-coupling superconductors like lead ( $T_c = 7.2$  K) or niobium ( $T_c = 9.25$  K). The phenomenon of high- $T_c$  superconductivity occurs for hole- and electron-doped cuprates in the vicinity of an antiferromagnetic phase transition. This suggests a purely electronic or magnetic mechanism in contrast to the conventional picture of electrons paired through the exchange of phonons. The simplest idea to explain such high critical temperature might be to introduce a higher cut-off energy  $\omega_c$  due to electronic correlations in the system instead of integrating over an energy shell of  $\omega_D$  (Debye frequency), i.e.  $T_c \propto \omega_c \exp(-1/\lambda)$ , where  $\lambda$  denotes the usual coupling strength for a given symmetry of the gap function. In the BCS theory [7]  $\lambda$  is equal to  $N(0)V$ , where  $N(0)$  is the density of states (per spin) at the Fermi level and where  $V = \text{const.}$  is the attractive pairing potential in  $\mathbf{k}$ -space acting between electrons leading to the superconducting instability of the normal state. If the relevant energy cut-off  $\omega_c$  of the problem is of the order of *electronic* degrees of freedom, e.g.  $\omega_c \simeq 0.3$  eV  $\approx 250$  K [8], one can easily obtain a transition temperature of the order of 100 K. However, as we will discuss below, in a more realistic treatment the relation between  $T_c$  and  $\lambda$  is, of course, not that simple.

Many researchers believe that in order to find the origin of the high- $T_c$

superconductivity in the cuprates it is necessary to investigate their normal state as a function of the doping concentration. Therefore, phenomenological models like the Marginal-Fermi-Liquid (MFL) [9], the Nested-Fermi-Liquid (NFL) [10,11] and the Nearly Antiferromagnetic Fermi Liquid (NAFL) theory [12] have been developed in order to understand the unusual non-Fermi liquid properties in the normal state. We will see later that our FLEX-theory provides a microscopic justification for these theories. In particular, in the underdoped regime of high- $T_c$  superconductors, i.e. closer to the antiferromagnetic transition than for optimal doping, a number of physical quantities exhibit quite unusual properties. Examples are the  $^{63}\text{Cu}$  spin-lattice relaxation rate and the inelastic neutron scattering intensity: while in the overdoped regime  $1/T_1T$  increases monotonously as  $T$  decreases down to  $T_c$ , one finds in the underdoped case that  $1/T_1T$  passes through a maximum at a temperature  $T^*$  (for decreasing  $T$ ) [13]. These results are fully corroborated by inelastic neutron scattering data, where in the underdoped regime  $\text{Im } \chi(\mathbf{Q}, \omega)$  at fixed small  $\omega$  ( $\simeq 10\text{-}15$  meV) passes also through a maximum at  $T^*$  for decreasing  $T$  [14]. In addition, angle-resolved photoemission experiments [15,16] on underdoped  $\text{Bi}_2\text{Sr}_2\text{CaCu}_2\text{O}_{8+\delta}$  indicate a presence of a gap with  $d_{x^2-y^2}$ -wave symmetry above  $T_c$  also in the charge-excitation-spectrum even up to room temperature. Recently, several experiments including heat capacity [17], transport [18], Raman scattering [19], and, in particular, scanning tunneling microscopy [20,21] indicate the existence of a gap in the excitation spectrum of the single-particle properties. This gap in the charge-response of the system occurs at the same temperature where also the spin gap opens. Therefore, this gap is then called “(weak) pseudogap”. One believes both gaps might have the same origin. Due to the  $d$ -wave symmetry of the pseudogap many researchers believe that it is related to precursor effects of the superconducting state [22,23]. In connection with simple arguments on the quasi two-dimensional nature of the system (see e.g. the theorem of Hohenberg [24]) these ideas suggest a non-trivial mechanism of the unusual behavior of underdoped cuprates. Thus, one of the main theoretical questions is to explain the origin of this weak pseudogap in the normal state and its relation to the underlying pairing mechanism.

Another fundamental problem to solve is the theoretical determination of the superconducting transition temperature  $T_c$  itself. A schematic phase diagram for hole-doped superconductors is shown in Fig. 1. At around  $x = 0.15$  one finds the highest  $T_c$  values. This region is called optimal doping. In the overdoped region, i.e.  $x > 0.15$ , many experimental data suggest that

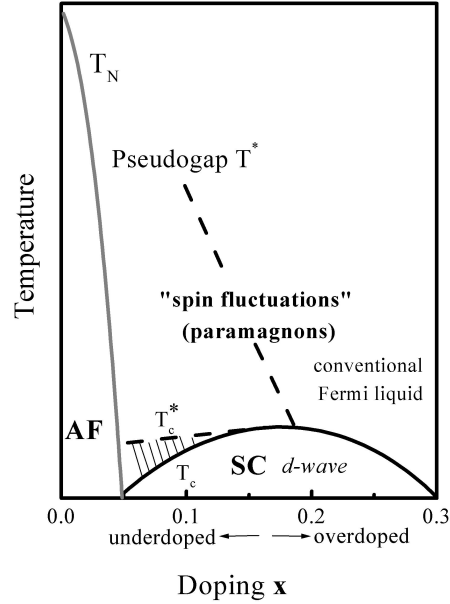


Figure 1. Schematic phase diagram of hole-doped cuprates [25]. High- $T_c$  superconductivity occurs in the vicinity of an antiferromagnetic phase transition. The corresponding superconducting order parameter is of  $d$ -wave symmetry. In the overdoped region, i.e.  $x > 0.15$ , the system behaves like a conventional Fermi liquid, whereas in the underdoped regime below the pseudogap temperature  $T^*$  one finds strong antiferromagnetic (AF) correlations. As we will discuss below, Cooper-pairing can mainly be described by the exchange of AF spin fluctuations (often denoted as paramagnons) which are present everywhere in the system. The doping region between  $T_c$  and  $T^*$  (shaded region) is due to local Cooper-pair formation. Below  $T_c$  these pairs become phase coherent.

the system is a conventional Fermi liquid. On the underdoped side of the phase diagram in contrast it is believed that below a mean-field transition temperature  $T_c^*$  one finds pre-formed Cooper-pairs without long-range phase coherence. This part of the phase diagram is sometimes called the “strong pseudogap” region. Below  $T_c$  these pairs become phase coherent and a Meissner effect of the bulk material is observed. Furthermore, in the experiment  $T_c \propto n_s$  is found only in underdoped superconductors [26]. So far, this has been mainly described in terms of the Ginzburg-Landau theory [22,23,27–29]. Recently, a microscopic calculation confirmed and clarified the picture [30].

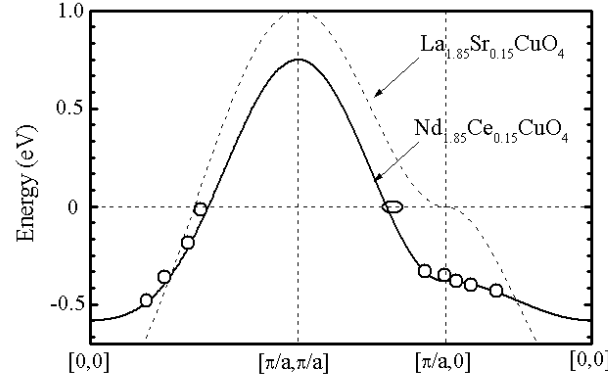


Figure 2. Results of the energy dispersion  $\epsilon_k$  of optimally hole-doped  $\text{La}_{1.85}\text{Sr}_{0.15}\text{CuO}_4$  (dashed line) and of optimally electron-doped  $\text{Nd}_{1.85}\text{Ce}_{0.15}\text{CuO}_4$  (NCCO). The solid curve refers to our tight-binding calculation choosing  $t = 138$  meV and  $t' = 0.3$ . Data (open dots) are taken from Ref. [31]. The dashed curve corresponds to using  $t = 250$  meV and  $t' = 0$  and is typical for hole-doped cuprates.

## 2 Theory of Cooper-Pairing by Antiferromagnetic Spin Fluctuations

### 2.1 Hubbard Model

In order to obtain a unified theory for both hole-doped and electron-doped cuprates we use the same one-band Hubbard Hamiltonian taking into account the different dispersions for the carriers [31]. When doping the electrons, they occupy copper  $d$ -like states of the upper Hubbard band while the holes refer to oxygen-like  $p$ -states yielding different energy dispersion as used in our calculations. Thus, assuming similar itinerancy of the electrons and holes, the mapping on an effective one-band model seems to be justified. We consider  $U$  as an effective Coulomb interaction.

On a square lattice the Hamiltonian  $H$  reads in second quantization

$$H = - \sum_{\langle ij \rangle \sigma} t_{ij} (c_{i\sigma}^\dagger c_{j\sigma} + c_{j\sigma}^\dagger c_{i\sigma}) + U \sum_i n_{i\uparrow} n_{i\downarrow} - \mu t \sum_{i\sigma} n_{i\sigma}, \quad (1)$$

where  $c_{i\sigma}^\dagger$  ( $c_{i\sigma}$ ) creates (annihilates) an electron on site  $i$  with spin  $\sigma$  and  $t_{ij}$  is a hopping matrix element. The sum performed over nearest neighbors is denoted by  $\langle ij \rangle$ . Then,  $t_{ij}$  is equal to  $t$ .  $U$  is the intra-orbital (i.e. on-site) Coulomb repulsion and  $n_{i\sigma}$  is equal to  $c_{i\sigma}^\dagger c_{i\sigma}$ .  $\mu$  denotes the chemical

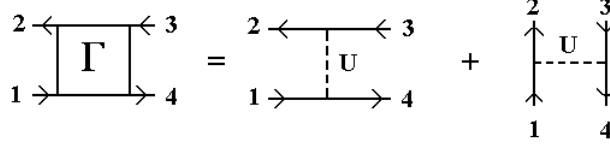


Figure 3. Antisymmetric four-point vertex-function  $\Gamma(1, 2, 3, 4)$ . The solid lines represent the electron propagators and the dashed line represents the on-site interaction  $U$ , respectively.

potential. Therefore, this model can be characterized by two dimensionless parameters, namely  $U/t$  and  $\mu$ .

Using Bloch wave functions we rewrite Eq. (1) as

$$H = \sum_{\mathbf{k}\sigma} \epsilon_{\mathbf{k}} c_{\mathbf{k}\sigma}^{\dagger} c_{\mathbf{k}\sigma} + \frac{1}{2} \frac{U}{N} \sum_{\mathbf{k}, \mathbf{k}', \mathbf{q}, \sigma} c_{\mathbf{k}\sigma}^{\dagger} c_{\mathbf{k}', -\sigma}^{\dagger} c_{\mathbf{k}'+\mathbf{q}, -\sigma} c_{\mathbf{k}-\mathbf{q}, \sigma}, \quad (2)$$

where the one-band electron dispersion in the normal-state  $\epsilon_{\mathbf{k}}$  reads for its nearest neighbor

$$\epsilon_{\mathbf{k}} = -2t [\cos k_x - \cos k_y + \mu/2] \quad (3)$$

and for next-nearest neighbor hopping

$$\epsilon_{\mathbf{k}} = -2t [\cos k_x - \cos k_y - 2t' \cos k_x \cos k_y + \mu/2], \quad (4)$$

respectively. Here,  $N$  is the number of lattice sites. As mentioned earlier, the bandstructure in Eq. (3) describes the Fermi surface of  $\text{La}_{2-x}\text{Sr}_x\text{CuO}_4$  [32], whereas for  $B = 0.45$ , Eq. (4) resembles the Fermi surface of  $\text{YBa}_2\text{Cu}_3\text{O}_{7-\delta}$  [33].

In order to discuss the dispersion relation for electron-doped cuprates in more detail, we show experimental results in Fig. 2 as well as our tight-binding calculation. We choose the parameters  $t = 138$  meV and  $t' = 0.3$ . For comparison we also show the results with  $t = 250$  meV and  $t' = 0$  which are often used to describe the hole-doped superconductor  $\text{La}_{2-x}\text{Sr}_x\text{CuO}_4$ . One immediately sees the important difference: in the case of NCCO the flat band is approximately 300 meV *below* the Fermi level, whereas for the hole-doped case the flat band lies very close to it. Thus, as discussed later, using the resulting  $\epsilon_k$  in a spin-fluctuation-induced pairing theory we get a smaller  $T_c$  for electron-doped cuprates than for the hole-doped ones.

## 2.2 Pairing Theory

In contrast to the usual Eliashberg theory of strong-coupling superconductors [34,35] in which phonons are involved one has to develop a theory for the exchange of AF spin fluctuations. One possibility is to use the phenomenological ansatz originally introduced by Millis, Monien, and Pines [12] where the effective pairing interaction  $V_{eff}(\mathbf{q}, \omega)$  is of the Ornstein-Zernike form. However, we believe that a self-consistent description is required because electronic degrees of freedom not only condense into Cooper-pairs, but also create the pairing interaction. Thus, one has to generalize the Eliashberg equations on a microscopic basis.

As we have seen earlier, the nearness to a spin-density-wave instability corresponds to a simple physical picture, in which the spins have short-range antiferromagnetic order surviving from the long-range order of the insulating phase. In terms of the Hubbard Hamiltonian the exchange of longitudinal and transverse spin fluctuations gives rise to an effective electron-electron interaction (originally introduced by Berk and Schrieffer [36]) that provides a pairing interaction leading to  $d$ -wave superconductivity near half filling. The effective paramagnon-like interaction then reads

$$V_{eff}(\mathbf{q}, i\nu_m) = \frac{3}{2}U^2 \frac{\chi_0(\mathbf{q}, i\nu_m)}{1 - U\chi_0(\mathbf{q}, i\nu_m)} - \frac{1}{2}U^2 \frac{\chi_0(\mathbf{q}, i\nu_m)}{1 + U\chi_0(\mathbf{q}, i\nu_m)}. \quad (5)$$

In order to solve the generalized Eliashberg equations we will use a self-consistent theory called FLuctuation-EXchange (FLEX) approximation [37,38]. Remember that the Hubbard-Hamiltonian can be rewritten in the form  $H = H_0 + H_{int}$ , where  $H_0$  describes the one-particle properties and  $H_{int}$  denotes a perturbation [39]. Let us start with introducing the antisymmetric four-point vertex-function  $\Gamma(1, 2, 3, 4)$  (see Fig. 3) [40] as  $\Gamma(1, 2, 3, 4) = V(1, 2, 3, 4) - V(1, 4, 3, 2)$ . The antisymmetry corresponds to a sign change in  $\Gamma$  after permuting the creation (annihilation) operators 2 (1) and 4 (3) due to the fact that no distinction can be made between identical electrons. With the help of  $\Gamma$  it is now possible to write down the corresponding self-energies of the conducting holes or electrons:

$$\begin{aligned}\Sigma^G &= \text{[Diagram 1]} + \text{[Diagram 2]} + \text{[Diagram 3]} + \dots \\ \Sigma^F &= \text{[Diagram 4]} + \text{[Diagram 5]} + \text{[Diagram 6]} + \dots\end{aligned}$$

The diagrams represent various self-energy contributions. Diagram 1 is a single vertex  $\Gamma$  with a loop. Diagram 2 is two vertices  $\Gamma$  connected by a horizontal line with a loop above. Diagram 3 is two vertices  $\Gamma$  connected by a horizontal line with a loop above and a vertical line between them. Diagram 4 is a single vertex  $\Gamma$  with a loop. Diagram 5 is two vertices  $\Gamma$  connected by a horizontal line with a loop above. Diagram 6 is two vertices  $\Gamma$  connected by a horizontal line with a loop above and a vertical line between them.

Here,  $\Sigma^G$  ( $\Sigma^F$ ) corresponds to the normal (anomalous) Green's function contribution. In order to solve these self-energy equations it is convenient to introduce the  $T$ -matrix [41] which is defined as

$$\text{[Diagram 7]} = \text{[Diagram 8]} + \text{[Diagram 9]} + \text{[Diagram 10]}$$

The diagrams represent the definition of the  $T$ -matrix. Diagram 7 is a box labeled  $T$  with four external lines. Diagram 8 is a box labeled  $\Gamma$  with four external lines. Diagram 9 is a box labeled  $\Gamma$  connected to a box labeled  $T$  by two vertical lines. Diagram 10 is a box labeled  $\Gamma$  connected to a box labeled  $\Gamma$  by two vertical lines.

Within the Nambu notation one arrives after a straightforward calculation at

$$\begin{aligned}\Sigma^G(\mathbf{k}, i\omega_n) &= \frac{1}{\beta N} \sum_{\mathbf{k}', i\omega'_n} \left[ \frac{1}{2} U^2 \frac{\chi_{s0}(\mathbf{q}, i\nu_m)}{1 + U\chi_{s0}(\mathbf{q}, i\nu_m)} + \frac{3}{2} U^2 \frac{\chi_{s0}(\mathbf{q}, i\nu_m)}{1 - U\chi_{s0}(\mathbf{q}, i\nu_m)} \right. \\ &\quad \left. + U^2 \chi_G(\mathbf{q}, i\nu_m) + U \right] G(\mathbf{k}', i\omega'_n),\end{aligned}\quad (6)$$

$$\begin{aligned}\Sigma^F(\mathbf{k}, i\omega_n) &= -\frac{1}{\beta N} \sum_{\mathbf{k}', i\omega'_n} \left[ \frac{1}{2} U^2 \frac{\chi_{s0}(\mathbf{q}, i\nu_m)}{1 + U\chi_{s0}(\mathbf{q}, i\nu_m)} - \frac{3}{2} U^2 \frac{\chi_{s0}(\mathbf{q}, i\nu_m)}{1 - U\chi_{s0}(\mathbf{q}, i\nu_m)} \right. \\ &\quad \left. - U^2 \chi_F(\mathbf{q}, i\nu_m) - U \right] F(\mathbf{k}', i\omega'_n),\end{aligned}\quad (7)$$

where  $i\nu_m = i\omega_n - i\omega'_n$ . Note that the term  $U^2 \chi_{G,F}$  on the right-hand side compensates double counting that occurs in the second order.  $\chi_{s0}$  and  $\chi_{c0}$  denote the irreducible spin- and charge-susceptibility, respectively, and are given by  $\chi_{s0}(q) = -\sum_k [G(k+q)G(k)F(k+q)F^\dagger(-k)] / \beta N$  and  $\chi_{c0}(q) = -\sum_k [G(k+q)G(k)F(k+q)F^\dagger(-k)] / \beta N$ , where  $q = (\mathbf{q}, i\nu_m)$  and  $k = (\mathbf{k}, i\omega_n)$ . The evaluation of the equations mentioned above are performed on the real axis [38,42]. In order to determine the superconducting transition temperature  $T_c$  we solve the linearized gap equation. Below  $T_c$  we find that the superconducting gap function has  $d_{x^2-y^2}$ -wave symmetry. Vertex corrections for the two-particle correlation function which are not included have been discussed elsewhere [42].



### 3 Results and Discussion

Let us start with the normal state of hole-doped cuprates. In Fig. 4(a), we display the density of states for different doping concentrations  $x = 1 - n$ . We define  $\rho(\omega) \equiv N(\omega) = \sum_{\mathbf{k}} N(\mathbf{k}, \omega)$ , with the spectral function  $N(\mathbf{k}, \omega) = -\text{Im } G(\mathbf{k}, \omega + i\delta)/\pi$ . For a doping value of 20 percent we obtain a peak close to the Fermi energy ( $\omega = 0$ ). However, if one gets closer to the spin-density-wave (AF) instability spectral weight at the same frequency is suppressed, leading to a dip. The temperature for which this phenomenon occurs defines the pseudogap temperature  $T = T^*$ . Recently, this has indeed been found by scanning tunneling microscopy experiments within the normal state of underdoped  $\text{Bi}_2\text{Sr}_2\text{CaCu}_2\text{O}_{8+\delta}$ . This pseudogap corresponds also to the gap measured in the charge-excitation-spectrum in the optical conductivity and is also seen in angle-resolved photoemission (ARPES) experiments by Shen and others as mentioned earlier (see, for example, Ref. [43]).

Next we want to discuss the superconducting gap function  $\phi(\mathbf{k}, \omega)$  shown in Fig. 4(b) for a given temperature  $T = 48\text{K}$  obtained for an intermediate coupling strength  $U/t = 4$  and for various doping concentrations  $x$ . The corresponding  $T_c$  values are  $T_c = 50\text{ K}$ ,  $T_c = 63\text{ K}$ ,  $T_c = 60\text{ K}$  (from top to bottom). In order to demonstrate the strong momentum dependence of the superconducting gap we show only the static part ( $\omega = 0$ ) and, for simplicity, only 1/4 of the first Brillouin zone. Due to feedback-effects from the gap function on the dynamical spin susceptibility one obtains a solution for the superconducting order parameter which belongs to the  $d_{x^2-y^2}$  wave representation but which is not the simple basis function  $\psi(\mathbf{k}) = \cos(k_x) - \cos(k_y)$ . In other words, the appearance of higher harmonics in the gap equation  $\phi(\mathbf{k}, \omega)$  (see in particular  $x = 0.07$ ) is a result of the self-consistent treatment of the effective pairing interaction which is dominated, of course, by the dynamical spin susceptibility  $\chi(\mathbf{q}, \omega)$ .

In order to calculate the phase diagram for hole-doped superconductors we must also calculate the superfluid density  $n_s(x, T)/m$  self-consistently from the current-current correlation function and from the f-sum rule: the real part of the conductivity  $\sigma_1(\omega)$ , i.e.  $\int_0^\infty \sigma_1(\omega) d\omega = \pi e^2 n/2m$ , where  $n$  is the 3D electron density and  $m$  denotes the effective band mass for the tight-binding band considered.  $\sigma(\omega)$  is calculated in the normal and superconducting state using the Kubo formula [44]. Vertex corrections have been neglected. Physically speaking we are looking for the loss of spectral weight of the Drude peak at  $\omega = 0$  that corresponds to excited quasiparticles above the superconduct-

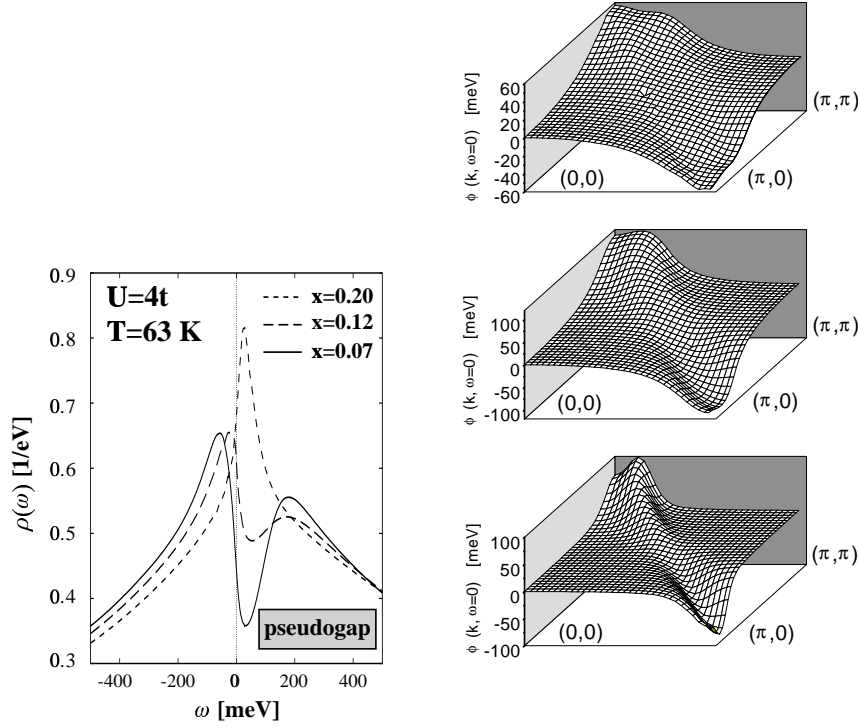


Figure 4. (a) Momentum averaged density of states  $\rho(\omega)$  for various doping concentrations. For large doping  $\rho(\omega)$  is similar to the uncorrelated case with a large van Hove singularity above the Fermi energy at  $\omega = 0$ . For small doping a pseudogap appears that is related to the antiferromagnetic correlations and a precursor of the spin density wave gap of a long-range ordered system. (b) Superconducting order parameter  $\phi(\mathbf{k}, \omega = 0)$  for various doping concentrations ( $x = 0.18$ ,  $x = 0.13$ ,  $x = 0.07$ , from top to bottom). All calculations are performed at  $T = 48\text{ K}$  using  $U = 4t$ . Note, the  $d$ -wave symmetry of  $\phi(\mathbf{k}, \omega = 0)$  and the appearance of higher harmonics in addition to the simple form  $\phi_{\mathbf{k}}^d = \phi_0[\cos(k_x) - \cos(k_y)]$  for underdoped systems.

ing condensate for temperatures  $T < T_c^*$ . Most importantly, using our results for  $n_s(x, T)$ , we calculate the doping dependence of the Ginzburg-Landau-like free-energy change  $\Delta F \equiv F_S - F_N$ , where  $\Delta F_{\text{cond}} \simeq \alpha(n_s/m)\Delta_0(x)$  is the condensation energy due to Cooper-pairing and  $\Delta F_{\text{phase}} \simeq \hbar^2/2m^*n_s$  the loss in energy due to phase incoherence of the Cooper-pairs. The parameter  $\alpha$  describes the available phase space for Cooper-pairs (normalized per unit volume) and can be estimated in the strongly overdoped regime. In the BCS-

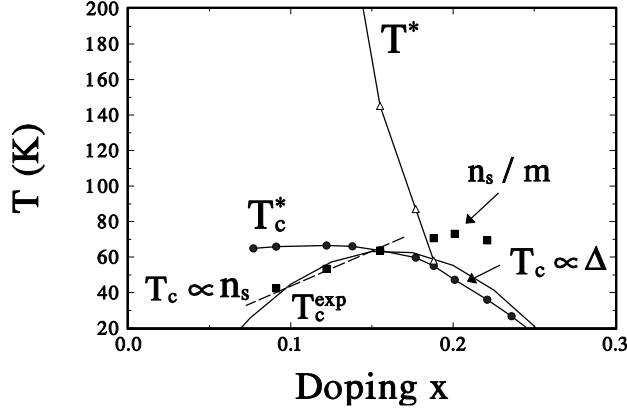


Figure 5. Phase diagram for hole-doped high- $T_c$  superconductors resulting from a spin fluctuation induced Cooper-pairing including their phase fluctuations. The calculated values for  $n_s(T = 0)/m$  are in good agreement with muon-spin rotation experiments.  $T_c^*$  denotes the temperature below which Cooper-pairs are formed. The dashed curve gives  $T_c \propto n_s(T = 0, x)$ . Below  $T^*$  we get a gap structure in the spectral density which is shown in Fig. 4(a).

limit one finds  $\alpha \simeq 1/400$ .  $\Delta_0$  is the superconducting order parameter at  $T = 0$ . Note,  $T_c$  and in particular  $T_c \propto n_s$  follows also from  $\langle n_s \rangle = 0$ , where one averages over the phase fluctuation time.

In Fig. 5 we show the resulting doping dependence of  $T_c(x)$ . We also display our results for the doping dependence of  $n_s(0)/m$ , which are in good agreement with experimental results. The curve  $T_c^{\text{exp}}$  describes many classes of cuprate material (it is taken from Loram and co-workers [45]). We would like to emphasize that, for the underdoped cuprates,  $T_c \propto n_s$  yields indeed better agreement with experimental results than  $T_c^*$  obtained from  $\Delta(x, T) = 0$  which mark the onset of Cooper-pairing within our mean-field theory. For the temperatures  $T_c < T < T_c^*$ , one finds pre-formed Cooper-pairs. For the overdoped cuprates, i.e.  $x > 0.15$ , we get largely BCS-type behavior and  $T_c \simeq T_c^* \propto \Delta$ . Hence, our electronic theory yields in fair agreement with experiment the non-monotonic doping dependence of  $T_c(x)$ . Note, we find similar results for the doping dependence of  $T_c$  from determining  $T_c$  using  $n_s(x, T) = 0$ . Here, one must include the coupling between Cooper-pairs and their phase fluctuations causing the reduction of  $T_c^* \rightarrow T_c$  for the underdoped cuprates and  $T_c \propto n_s$ . In Fig. 5 results are also given for the characteristic temperature  $T^*$  at which a gap appears in the spectral density. Within

our FLEX-theory the occurrence of a pseudogap is due to inelastic electron-electron scattering which leads to a loss of spectral weight at the Fermi level. These are in qualitative agreement with experiments. Finally, we calculate also  $T_c$  for the underdoped cuprates with  $n_s(T)$  and the Kosterlitz-Thouless theory [46],  $k_B T_c(x) = \hbar^2 n_s(T_c)/4ma$  with  $a = 2/\pi$ , and have found similar  $T_c$  values.

We also calculate the phase diagram  $T_c(x)$  and  $T_N(x)$  of electron-doped cuprates. In order to obtain a unified theory for both hole-doped and electron-doped cuprates it is tempting to use the same Hubbard Hamiltonian taking of course into account the different dispersions for the carriers. Note, in the case of electron doping the electrons occupy copper  $d$ -like states of the upper Hubbard band while the holes refer to oxygen-like  $p$ -states yielding different energy dispersion as used in our calculations. Then, assuming similar itinerancy of the electrons and holes the mapping on an effective one-band model seems to be justified. We consider  $U$  as an effective Coulomb interaction. We find in comparison to hole-doped superconductors smaller  $T_c$  values and that superconductivity occurs in a narrower doping range as also observed in experiment. Responsible for this are poorer nesting properties of the Fermi surface and the flat band around  $(\pi, 0)$  which lies well below the Fermi level. The narrow doping range for  $T_c$  is due to antiferromagnetism up to  $x = 0.13$  and rapidly decreasing nesting properties for increasing  $x$  [47]. In order to understand the behavior of  $T_c(x)$  in underdoped electron-doped cuprates we have calculated the Cooper-pair coherence length  $\xi_0$ , i.e. the size of a Cooper-pair, and find similar values for electron-doped and hole-doped superconductors (from 6 Å to 9 Å). If the superfluid density  $n_s/n$  becomes small (for example due to strong coupling lifetime effects), the distance  $d$  between Cooper pairs increases. If for  $0.15 > x > 0.13$  the Cooper-pairs do not overlap significantly, i.e.  $d/\xi_0 > 1$ , then Cooper-pair phase fluctuations get important. Thus we expect like for hole-doped superconductors  $T_c \propto n_s$ . Below  $T_c$  we find for all doping concentrations that the gap function has clearly  $d_{x^2-y^2}$ -wave symmetry. This is in agreement with the reported linear and quadratic temperature dependence of the in-plane magnetic penetration depth for low temperatures in the clean and dirty limit, respectively, and with phase-sensitive measurements [4]. Previous experiments did not clearly support this and reported mainly  $s$ -wave pairing. Maybe as a result of this, so far electron-doped cuprates received much less attention than hole-doped cuprates.

## 4 Summary

We have used the Hubbard Hamiltonian and the self-consistent FLEX-theory as a model to calculate some basic properties of the hole-doped and electron-doped cuprate superconductors. For the hole-doped case we have discussed the superfluid density  $n_s/m$ , and the critical temperature  $T_c$  as a function of the doping concentration. We found a phase diagram with two different regions: on the overdoped side a mean-field-like transition and  $T_c \propto \Delta(T=0)$ , and on the underdoped regime  $T_c \propto n_s(T=0)$ . For temperatures  $T_c < T < T_c^*$  there is a finite superfluid density, but no Meissner effect. This region may be attributed to pre-formed Cooper-pairs without long-range phase coherence. Above  $T_c^*$  one has a third energy scale, namely  $T^*$  with a gap below in the spectral density of states (“pseudogap”).

Our unified model for cuprate superconductivity yields for electron-doped cuprates like for hole-doped ones pure  $d_{x^2-y^2}$  symmetry pairing in a good agreement with recent experiments [4]. In contrast to hole-doped superconductors we find smaller  $T_c$  values for electron-doped cuprates due to a flat dispersion  $\epsilon_k$  around  $(\pi, 0)$  well below the Fermi level. Furthermore, superconductivity occurs only for a narrow doping range  $0.18 > x > 0.13$ , because of the onset of antiferromagnetism and, on the other side, due to poorer nesting conditions. We get  $2\Delta/k_B T_c = 5.3$  for  $x = 0.15$  for the electron-doped cuprates, whereas we obtain much larger values for the hole-doped ones, namely  $2\Delta/k_B T_c = 10-12$ . The overall agreement with experiments on hole- and electron-doped high- $T_c$  superconductors is remarkably good and suggests spin-fluctuation exchange as the dominant pairing mechanism for superconductivity.

## Acknowledgments

It is a pleasure to thank H. Kleinert, A. Pelster, I. Eremin, and C. Joas for helpful discussions. In particular, K.H. Bennemann likes to thank H. Kleinert for more than 20 years of friendly and inspiring colleagueship and many discussions.

## References

- [1] J.G. Bednorz and K.A. Müller, *Z. Phys. B* **64**, 189 (1986).

- [2] B. Stadlober *et al.*, *Phys. Rev. Lett.* **74**, 4911 (1995).
- [3] S.M. Anlage *et al.*, *Phys. Rev. B* **50**, 523 (1994).
- [4] C.C. Tsuei and J.R. Kirtly, *Phys. Rev. Lett.* **85**, 182 (2000).
- [5] J.D. Kokales *et al.*, *Phys. Rev. Lett.* **85**, 3696 (2000).
- [6] R. Prozorov, R.W. Gianetta, P. Fournier, and R.L. Greene, *Phys. Rev. Lett.* **85**, 3700 (2000).
- [7] J. Bardeen, L.N. Cooper, and J.R. Schrieffer, *Phys. Rev. B* **108**, 1175 (1957).
- [8] J. Ruvalds *et al.*, *Phys. Rev. B* **51**, 3797 (1995).
- [9] C.M. Varma *et al.*, *Phys. Rev. Lett.* **63**, 1996 (1989).
- [10] A. Virosztek and J. Ruvalds, *Phys. Rev. B* **42**, 4064 (1990).
- [11] J. Ruvalds, C.T. Rieck, J. Zhang, and A. Virosztek, *Science* **256**, 1664 (1992).
- [12] A.J. Millis, H. Monien, and D. Pines, *Phys. Rev. B* **42**, 167 (1990).
- [13] For a review, see C.P. Slichter in *Strongly Correlated Electronic Systems*, Eds. K.S. Bedell, Z. Wang, and D.E. Meltzer (Addison Wesley, Reading, MA, 1994).
- [14] L.P. Regnault *et al.*, *Physica B* **213-214**, 48 (1995).
- [15] D.S. Marshall *et al.*, *Phys. Rev. Lett.* **76**, 4841 (1996).
- [16] J.M. Harris *et al.*, *Phys. Rev. B* **54**, R15655 (1996).
- [17] J.W. Loram, K.A. Mirza, J.R. Cooper, and W.Y. Liang, *Phys. Rev. Lett.* **71**, 1740 (1993); J.W. Loram *et al.*, *J. Superconductivity* **7**, 243 (1994).
- [18] B. Batlogg *et al.*, *Physica C* **235-240**, 130 (1994).
- [19] R. Nemeschek *et al.*, *Phys. Rev. Lett.* **78**, 4837 (1997); G. Blumberg *et al.*, *Science* **278**, 1427 (1997).
- [20] C. Renner *et al.*, *Phys. Rev. Lett.* **80**, 149 (1998).
- [21] A.K. Gupta and K.-W. Ng, *Phys. Rev. B* **58**, R8901 (1998).
- [22] B.K. Chakraverty, A. Taraphder, and M. Avignon, *Physica C* **235-240**, 2323 (1994); B.K. Chakraverty and T.V. Ramakrishnan, *Physica C* **282-287**, 290 (1997).
- [23] V.J. Emery and S.A. Kivelson, *Nature* **374**, 434 (1995).
- [24] P.C. Hohenberg, *Phys. Rev.* **158**, 383 (1967).
- [25] J.L. Tallon, *Phys. Rev. B* **51**, 12911 (1995).
- [26] Y.J. Uemura *et al.*, *Phys. Rev. Lett.* **62**, 2317 (1989).
- [27] H. Kleinert, *Gauge Fields in Condensed Matter*, Vol. I: *Superflow and Vortex Lines* (World Scientific, Singapore, 1989).

- [28] H. Kleinert and E. Babaev, *Phys. Rev. B* **59**, 12083 (1999).
- [29] A.K. Nguyen and A. Sudbø, *Phys. Rev. B* **60**, 15307 (1999).
- [30] D. Manske and K.H. Bennemann, *Physica C* **341-348**, 83 (2000).
- [31] D.M. King *et al.*, *Phys. Rev. Lett.* **70**, 3159 (1993).
- [32] Q. Si, Y. Zha, K. Levin, and J.P. Lu, *Phys. Rev. B* **47**, 9055 (1993).
- [33] J.C. Campuzano *et al.*, *Phys. Rev. Lett.* **64**, 2308 (1990).
- [34] G.M. Eliashberg, *Sov.-Phys.-JETP* **11**, 696 (1960).
- [35] P.B. Allen and B. Mitrovic, *Solid State Physics* **37**, 1 (1982).
- [36] N.F. Berk and J.R. Schrieffer, *Phys. Rev. Lett.* **17**, 433 (1966).
- [37] N.E. Bickers, D.J. Scalapino, and S.R. White, *Phys. Rev. Lett.* **62**, 961 (1989); N.E. Bickers and D. J. Scalapino, *Ann. Phys. (N.Y.)* **193**, 206 (1989); P. Monthoux and D.J. Scalapino, *Phys. Rev. Lett.* **72**, 1874 (1994); C.-H. Pao and N.E. Bickers, *Phys. Rev. Lett.* **72**, 1870 (1994).
- [38] T. Dahm and L. Tewordt, *Phys. Rev. Lett.* **74**, 793 (1995); *Phys. Rev. B* **52**, 1297 (1995).
- [39] D.J. Scalapino, *Phys. Rep.* **250**, 329 (1995).
- [40] A.A. Abrikosov, L. Gorkov, and I.E. Dzyaloshinskii, *Quantum Field Theoretical Methods in Statistical Physics* (Pergamon Press, Oxford, 1965).
- [41] L. Tewordt, D. Fay, P. Dörre, and D. Einzel, *J. Low Temp. Phys.* **21**, 645 (1975).
- [42] D. Manske, *Phonons, Electronic Correlations, and Self-Energy Effects in High- $T_c$  Superconductors*, PhD thesis, Hamburg, Germany, 1997 (Shaker Verlag, Aachen, 1997).
- [43] Z.X. Shen and D.S. Dessau, *Phys. Rep.* **253**, 1 (1995).
- [44] S. Wermbter and L. Tewordt, *Physica C* **211**, 132 (1993).
- [45] M.R. Presland *et al.*, *Physica C* **176**, 95 (1991); J.R. Cooper and J.W. Loram, *J. Phys. (France) I* **6**, 1 (1996).
- [46] J.M. Kosterlitz and D.J. Thouless, *J. Phys. C* **6**, 1181 (1973); J.M. Kosterlitz, *J. Phys. C* **7**, 1046 (1974).
- [47] D. Manske, I. Eremin, and K.H. Bennemann, *Phys. Rev. B* **62**, 13922 (2000).